ACCEPTABILITY OF DYNAMIC FINITE ELEMENT ANALYSES – MATERIAL FAILURE APPROACH

Anindya Sen
Her Majesty's Inspector
Department for Transport (Central)
Zone 2/26, Great Minster House,
76, Marsham Street, London, SW1P 4DR, UK
Ph: +44 (0)20 7944 2763
Email: anindya.sen@dft.gsi.gov.uk

DISCLAIMER

The views expressed here are those of the author/s and do not constitute official GB Competent Authority's policy statement

ABSTRACT

IAEA [701] details how compliance with the regulatory tests may be achieved. The GB Competent Authority has always been open minded to new calculation procedures and has encouraged the use of finite element analysis where appropriate. In the last few years there has been a marked increase in the complexity of some analyses, which support applications, with attempts made to model material failure in a conservative manner. We have noticed a range of failure theories and modelling methods that may, or may not be acceptable. This paper attempts to clarify our expectations with regard to modelling failure.

In elastic analyses, the main acceptance criterion is to check that the calculated stresses, e.g. Von-Mises or Tresca do not exceed the lower bound yield stress/es for the material/s. If the stresses exceed the yield limit/s, the determining criterion shifts from stress to strain; especially under multi-axial load conditions. Elastic-plastic analysis using finite element approach, solicits, true stress-strain curve for the material/s to be incorporated. The most relevant material property for comparison now is the available engineering uniaxial ductility. It is a global measure of failure, whereas, the local strains in the vicinity of the failure zone could be much higher. For a static analysis, the enumerated strains are available at the end of the analysis, whereas, in a dynamic analysis, the set period for analysis should be "long" enough to ensure that the response has been captured correctly at the end of the analysis. In most of the engineering applications, the state of stress is generally multi-axial, thus affecting the available ductility, which decreases non-linearly under predominant tensile multi-axial stress state. The elastic-plastic assessments need to show that to underwrite the integrity of a component, the final accumulated equivalent plastic strains are below the available multi-axial ductility for the respective material/s at the relevant temperature/s.

Extensive FE analyses related to regulatory requirements will be done. Comments will be made on mesh quality, input parameters and post-processing diagnostics in an attempt to guide the analyst to

a fit-for-purpose FE model. Finally, a quantifiable and recommendable margin when comparing the strains as stated above will be suggested.

INTRODUCTION

The operational robustness of a United Nations (UN) Class 7 Type B package (Ref.1) is checked by undertaking an impact test on an unyielding surface with a drop height of 9 m, considering its worst orientation. This is required by the IAEA document, TS-R-1 (Ref. 1) and reflected through the relevant UN and domestic regulatory documents. The current paper considers a simple representative Type B package subjected to an impact test and appraises its structural integrity using a multi-axial strain-based failure criterion for a representative ductile material. The primary objective of this paper is to allude the reader and the wider community towards the failure criterion while undertaking the impact assessments.

SYSTEM DESCRIPTION

The representative Type B package is assumed to be a thin walled (10mm) hollow (flat) end-capped cylinder of typical ductile carbon steel with an outer diameter of 300mm and a nominal length of 1200mm. The mass of the package has been calculated to be ~95 kg (Table 1). No internal radiation / thermal shielding and shock absorbing mechanisms have been considered. The total internal content (unspecified) has been assumed to weigh 13,754 N; (vertical) distributed equally at every node (1 kgf or 9.81 N at each of the 1402 nodes). This is to simplify modeling the internal content and is judged not to affect the package behaviour significantly. It is also judged that this representation is adequate for satisfying the objective of this paper. The conditions external and internal to the cylinder have been considered to be ambient and isothermal. In most of the cases with real packages, it has been observed that the worst orientation for the “drop test” from the “containment” integrity considerations is the one where the centre of gravity passes through one of the weakest (e.g. vicinity of “O” ring seal) corners. However, in the current study the package is assumed to be orientated at 45^{o} to the horizontal for ease of modeling purposes.

FINITE ELEMENT MODEL

The finite element model of the package has been developed using the Ansys12.1 (Ref. 2) graphical user interface (PREP7 GUI). The entire metallic shell of the package (Figure 1) has been modeled using LS-Dyna (Ref. 2) compatible linear “Shell 163” element, which is suitable for the explicit analysis. Three integration points (default) have been considered through the thickness. The package has been assumed to be positioned at an angle of 45^{o} to the horizontal and dropped from a height of 9.0 m (lower bottom corner) on an unyielding (rigid) surface. The rigid impacting surface has been defined in the model using the “rigid material” properties in LS-Dyna with appropriate degrees of freedom constrained. The interaction between the package and the rigid surface has been assumed to generate both static and dynamic friction effects and typical coefficients have been used (Table 1). General contact definitions were used for ease of modeling and various explicit algorithm tolerances were left to their default values. After some trials with the mesh density, the final mesh profile was judged to be adequate for the assessment purposes. No welds have been modeled.

The terminal velocity just before the impact has been calculated to be ~13.0 ms^{-1}. The impact analysis was set for 0.175 seconds, encompassing the impact, rebound, “slap-down” and progressively attenuating vibration after the event. This could be evident from the plots of various

energy histories for the model. The analysis was undertaken using a standard PC (Intel Core 2 Duo) with 3GB memory and MS Windows operating system (32 bit) executing "*ls971*" solver (Ref. 2).

MATERIAL DATA

The material used for the current package is a representative typical carbon steel. The physical and lower bound tensile properties have been taken from BS 1501: Part 1 (Ref. 3) for carbon steel plates (semi-killed with Aluminium) with thickness between 3.0-16.0 mm. For the current study, the package has been assumed to be at ambient temperature and all the physical (Table 1) and lower bound tensile (Table 2) properties are relevant accordingly. A bilinear true stress-strain data (*Mat_Plastic_Kinematic) have been used for the carbon steel without any limiting rupture strain data. As a strain based failure criterion is being used for the assessment, it is pessimistic to use the lower bound parent properties (no welds present).

ASSESSMENT PROCEDURE

The impact generally results in initial elastic response followed by progressive plastic deformation in the vicinity of the impacting zones. Since, the strains are expected to be predominantly plastic, hence, the integrity assessment must undertake a suitable "strain based acceptance" criterion. One such approach, which has been widely used and appreciated by the domestic nuclear industry is the "strain (and energy) acceptability" criterion in the R3 Impact Assessment procedure (Ref. 4). The basis of this criterion is the response of any ductile material (metal) under large strains; i.e., strains >> proof strains (e.g. 0.2% for carbon steel). It has been found that in plates, shells and solids; under multi-axial stress state (well above yield), "the equivalent strain at rupture is not equal to the uniaxial strain at rupture". Theoretically, it has been found that this variation is dependent on the relative magnitude of the hydrostatic tension, which can be expressed as the ratio of the mean (hydrostatic) stress to the equivalent multi-axial stress (e.g. Von-Mises), defined as the multi-axiality factor "*m*". For predominantly compressive stress state, the allowable rupture strain could theoretically be higher than the uniaxial rupture data, however, for all practical purposes, it is assumed (pessimistic) to be limited to the uniaxial rupture strain ε_u. The data from four structural steels under various multi-axial stress states have been plotted (best estimate fit) in R3 (Ref. 4). It is essentially a plot of the multi-axiality factor *m* along the abscissa (*x*) and the ratio of the (multi-axial) equivalent plastic strain to uniaxial rupture strain along the ordinate (*y*). For the current assessment, a fourth degree equation has been fitted to the R3 curve for ease of assessment and appropriate limits have been applied to reflect the philosophy correctly.

Upon completion of the analysis, the evolution of (integration point) equivalent plastic strains with time over the whole model is observed using LS Pre/Post tool (Ref. 2). The equivalent plastic strain (EPS) is the equivalent true strain output from the model, which needs to be compared with the "allowable" lower bound multi-axial strain. At first, the elements are identified undergoing plastic deformation, followed by extraction of stress and strain histories over the duration of "impact". The principal stresses are used to calculate the hydrostatic and Von-Mises stresses followed by the multi-axiality factor *m* at each time point for the identified elements. The *m* values are used in the equation to the R3 curve to calculate the "allowable" lower bound multi-axial rupture strains, which are now compared with the equivalent plastic strains for each element at each time point. For a particular element at a particular time point, the abscissa and the ordinate values can be plotted and checked against the "best fit" R3 curve, as would be shown later. If the plotted data remains bounded by the curve (i.e. inside) then the element pass the integrity assessment criterion, however,

if it falls outside, then the element is judged to have "failed". It is recommended to investigate the time histories of the stress resultants of such "failed" elements to check their real response and judge "failure" accordingly.

RESULTS

It was judged to have the outputs of various parameters at every 0.25E-03 s (*cf.* 0.175 s) for ease of post processing and due to some level of constraint with the file sizes. The simulated package dropped at the lower corner first, rebounded and then rotated to "slap-down" at the other end, continuing with some further secondary and tertiary impacts before coming to rest.

Energy Histories

The various energy histories for the whole model are plotted in Figure 2, which states that the choice of the duration of the analysis was more than adequate. The kinetic energy is observed to be falling with time along with progressive increase in the internal energy due to plastic deformation and external work done by the nodal forces (*cf.* 9.81 N at each node). After the rebound, the model rotates, while slapping down at the other end. This is reflected in the kinetic and internal energy histories. The internal energy curve reflects the strain energy accumulated in the plastic deformation of the elements during the impacts. It can be observed that the sliding energy due to work done against friction is fairly low and acceptable. All the energy history curves are stable after 0.1 s indicating that the primary impact was over much earlier. The total energy history [*TE(t)*] includes the effect of "external work" done by the nodal forces apart from the summation of other energies (Ref. 2). Since, the "external work" progressively increases with time, the total energy history goes up as well. This is an artifact of the interpretation of the energy histories only. If the reader interprets the external work as "potential energy" expended by the nodal forces, then it becomes easier to follow the conservative nature of the system, which is amply maintained at all time points.

Stresses and Strains

The impact generates a significant amount of plastic strains in the elements at both ends. A plot of the equivalent plastic strains in Figure 3 shows a representative snap shot during the whole impact scenario. The "slap-down" end has been picked in Figure 4 to elicit the plastic strain distribution. Two elements (451 & 452, Figure 4) with accumulated plastic strains have been chosen as representative ones to elucidate the procedure. The plastic strain histories of those two elements are shown in Figure 5, indicating that after the "slap-down", the plastic straining occurs very quickly with average strain rate of 400 s^{-1}. Various stress histories for the representative element 451 (integration point #3) have been plotted in Figure 6, where it can be observed that after the "slap-down", Von-Mises stress sharply reaches the yield stress and starts hardening up for a short period following the hardening modulus, before dropping quickly to an oscillatory trend with an mean of about 1.25+E08 Pa, with no further accumulation of plastic strains (Figure 5).

STRAIN BASED ASSESSMENT

The assessment procedure has been elucidated here using the results from integration points 1 and 3 of the representative element 451. In the case of real life assessments, the analyst needs to assess integrity of all the concerned elements (including the different integration points) using the strain based procedure. The stresses and strains for element 451 have been obtained at five consecutive time points so as to capture the transition from elastic to progressively plastic response during the actual impact. The stresses have been used to calculate the "*m*" factors at those identified time

points, while the respective equivalent plastic strain data have been divided by the lower bound uniaxial rupture strain to give the ordinate values corresponding to each "*m*" data point along the abscissa. The enumerated values are now plotted against the R3 curve to check for "failure", as defined earlier. For the element 451, it is observed from Figure 7 that immediately after the impact (Figure 2), when the plastic strain is still very small (Figure 5), the data points (for ip#1 & 3) remain well within the R3 curve. However, as the impact progressed, the equivalent plastic strains increased significantly without any significant change in the corresponding "*m*" data. Hence, rest of the calculated data points remain outside the R3 curve indicating "failure".

The stress history plots (Figure 6) for the element 451 shows that during and after the impact, the stresses continue to remain predominantly compressive. The plastic strains continue to be accumulated in the element up to a certain time point just after the impact, even well exceeding the lower bound ductility (Table 2). This is because of lack of any limiting strain data (i.e. rupture) for the bi-linear material curve (*Mat_Plastic_Kinematic) used in LS-Dyna. Hence, upon impact, the stresses and strains continue to increase elastically following the Young's Modulus E up to the Yield Stress σ_y, after which, the post yield response is determined by the monotonic hardening modulus E_t without any limit on stress (e.g. UTS) or strain (e.g. rupture). Although the stress state remains compressive, yet the accumulated equivalent plastic strain is well beyond the lower bound uniaxial ductility and it is deemed to have failed. The average strain rate during the very short duration actual impact period has been calculated to be about 400 s^{-1}. At this "high" strain rate, a real material will tend to harden up significantly and the actual strains are most likely to be much lower. Similar assessments have been carried out for element 452 but not presented here.

In case of another element 441 (ip#3), it is observed that after the impact, the stress state changes from compressive to significantly tensile and following Figure 8, it can be seen that as the "*m*" factor becomes increasingly positive, the R3 curve ordinate ratio decreases (<1.0) indicating that the allowable multi-axial strain at that point is less than the uniaxial ductility. However, the element still remains well within the R3 curve as can be seen from Figure 8.

This strain based assessment procedure needs to be repeated for all the elements with accumulated equivalent plastic strains. If this could be done within the post processing tool, it would expedite the procedure significantly. Otherwise, all the relevant output variables data need to be obtained from the analysis and the procedure needs to be followed for each element by some other means.

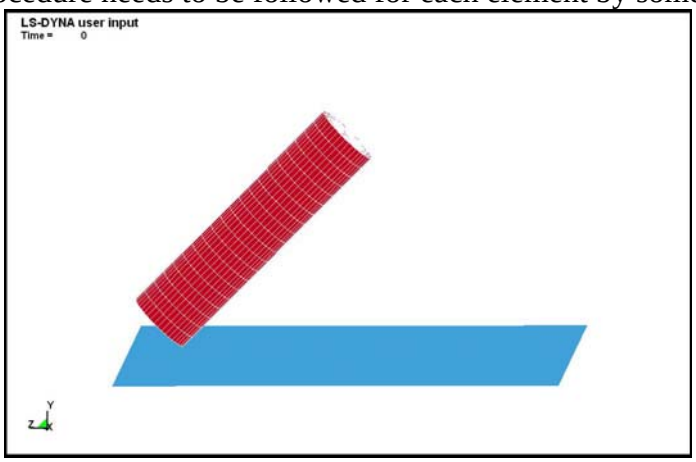

Figure 1: Representative Type B(U) Package with Postulated Drop Orientation

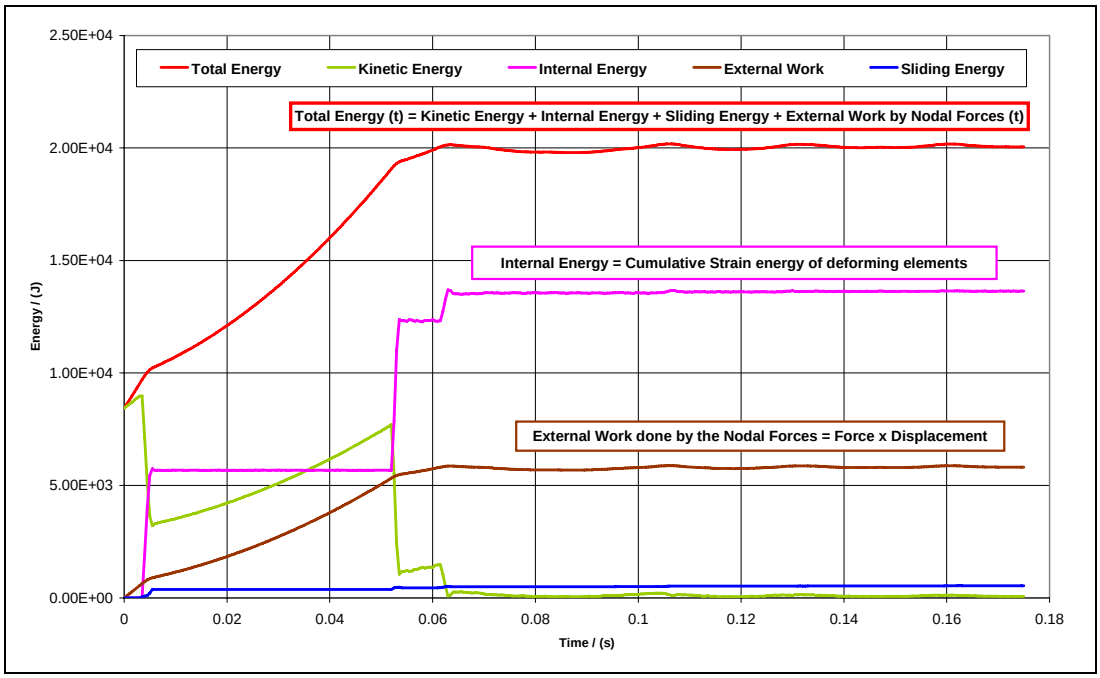

Figure 2: Overall Energy Histories

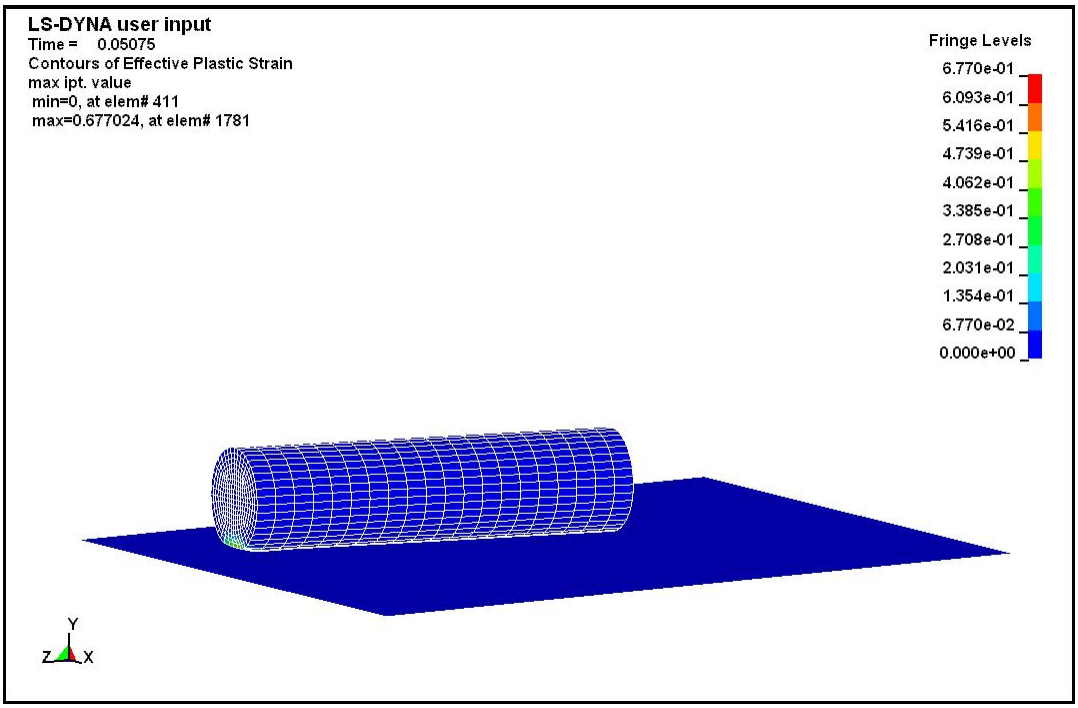

Figure 3: Equivalent Plastic Strain Distribution – "Snap Shot"

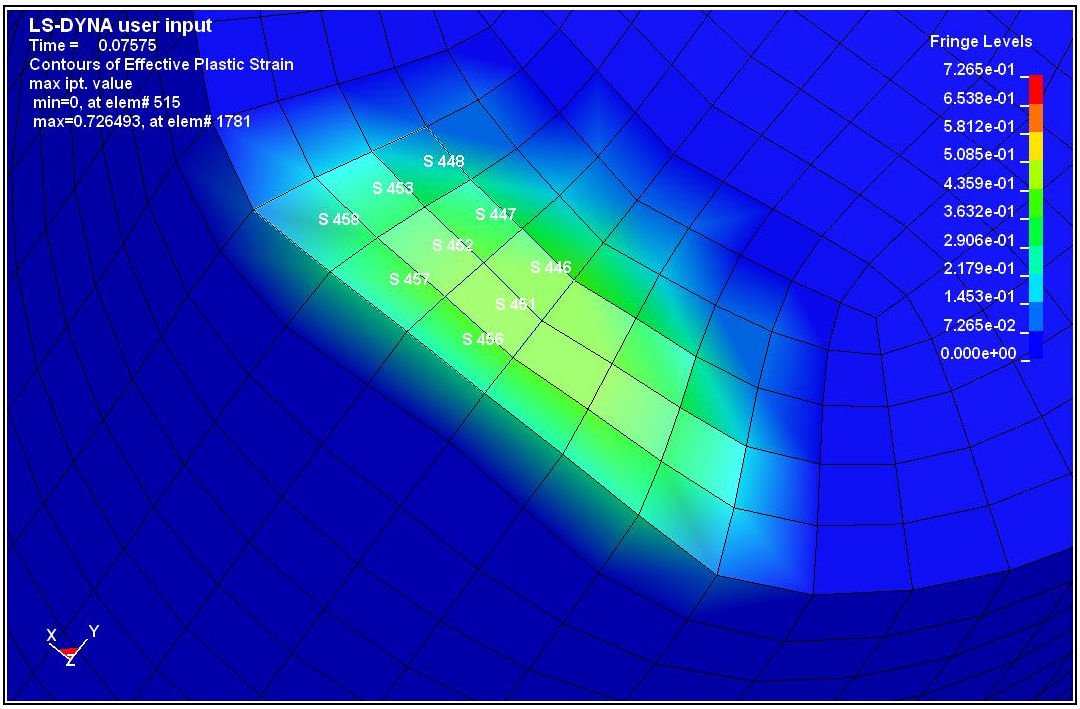

Figure 4: "Slap-down" End Elements with Plastic Strains

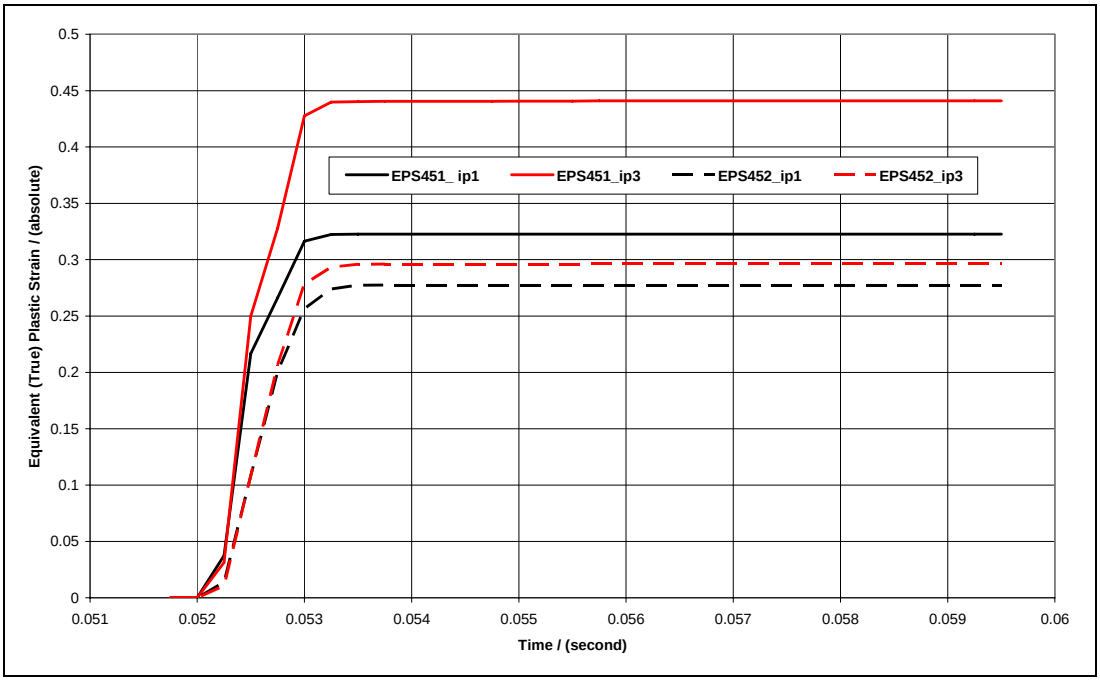

Figure 5: Equivalent Plastic Strain Histories for Elements 451 and 452

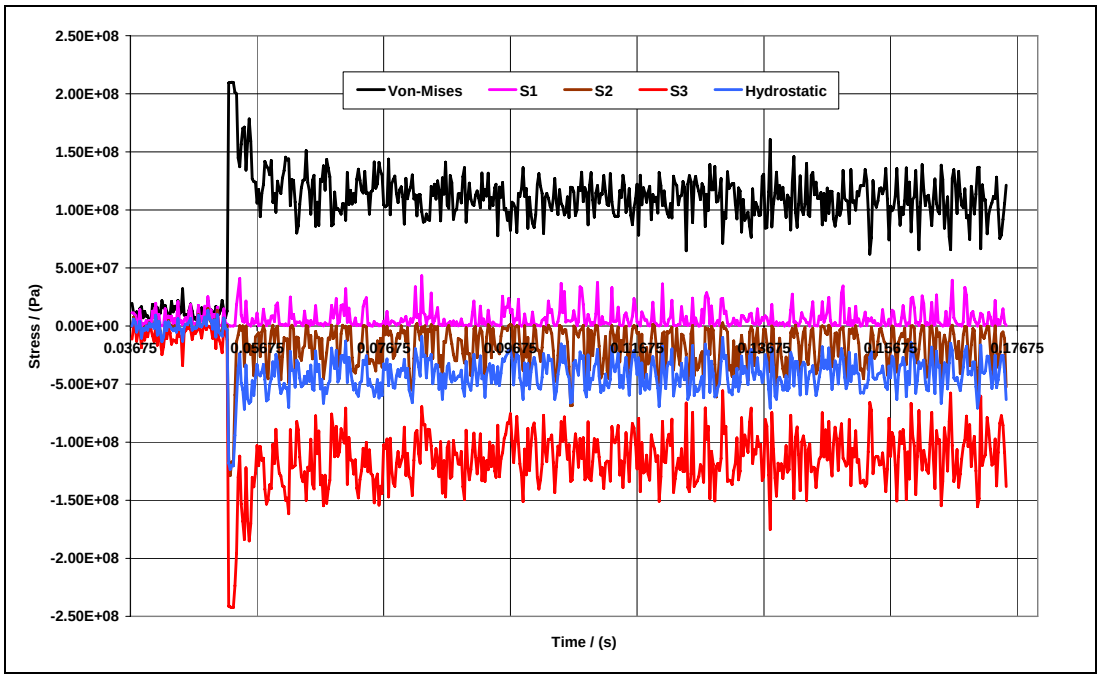

Figure 6: Stress Histories for Representative "Slap-Down" End Element 451 (ip#3)

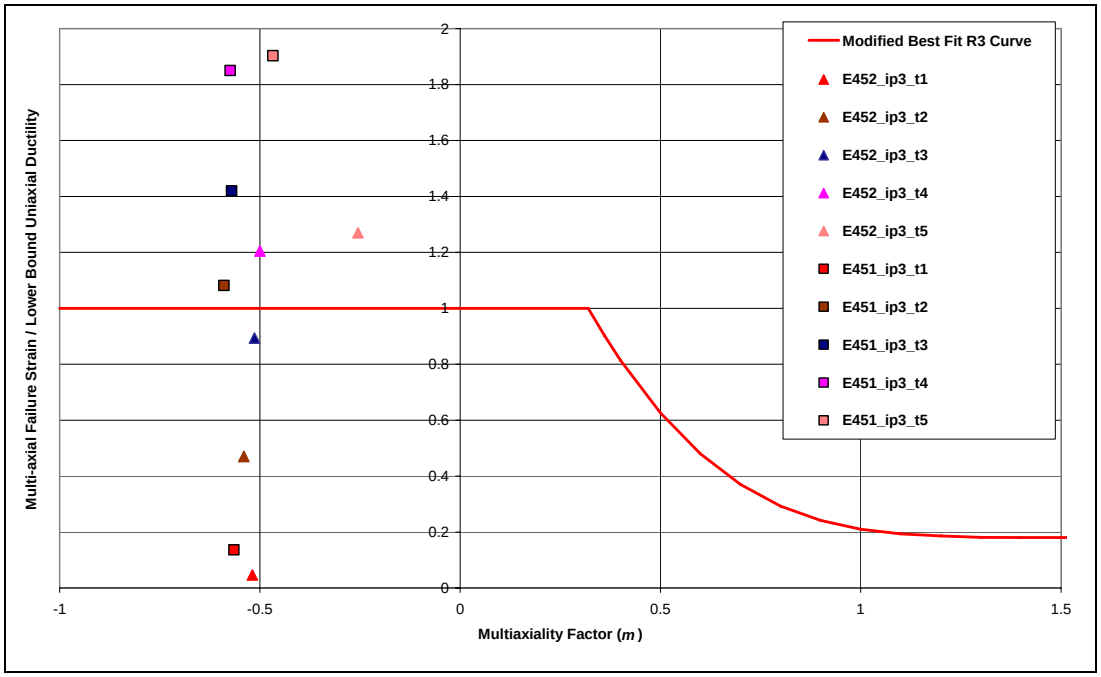

Figure 7: Typical Comparison with R3 Curve for Elements 451 (ip#1 & 3) With Time

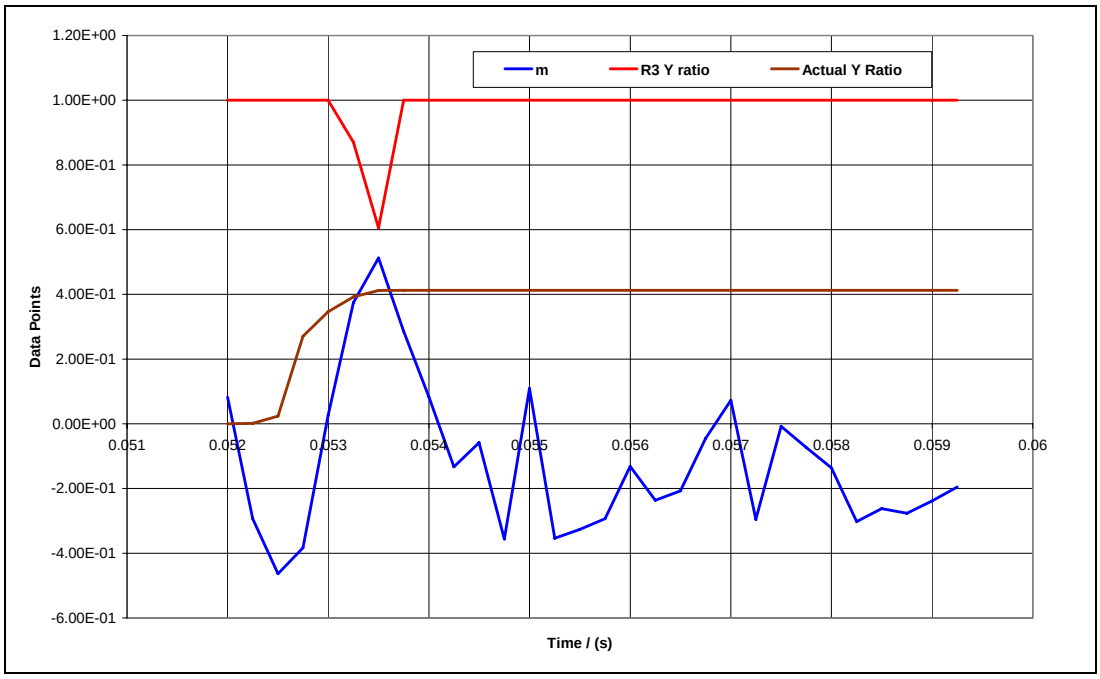

Figure 8: Typical Assessment Data Plots for Element 441 (#ip3)

Density ρ (kg/m^3)	Young's Modulus E (Pa)	Poisson's Ratio μ	Coefficient of Friction - Static μ_{static}	Coefficient of Friction - Dynamic $\mu_{dynamic}$
7850.0	0.21E+12	0.29	0.1	0.12

Table 1: Physical Properties and Typical Friction Data for Carbon Steel

Lower Bound Yield Stress σ_y (Pa)	Lower Bound Ultimate Tensile Strength σ_{UTS} (Pa)	Lower Bound Uniaxial Ductility ε_u (%)	Hardening Modulus E_t (Pa)
0.205E+09	0.360E+09	26.0	0.1075E+10

Table 2: Room Temperature Tensile Data for Typical Carbon Steel

CONCLUSIONS

The integrity of a representative Type B package has been assessed using the strain based procedure as described in R3 (Ref. 4). One representative element has been used to elucidate the various steps of the procedure. It has been found after the analysis that the element has failed because the accumulated plastic strain has significantly exceeded the lower bound uniaxial ductility, under compressive stress state. However, the strain rate has been calculated to be very high during the impact period, which for a real material would result in considerable hardening and would most likely reduce the accumulated plastic strains significantly.

There is adequate pessimism in the assessment by using the lower bound materials data and ignoring strain rate based work hardening, while using bilinear stress-strain curve for FE analysis. No shock absorbing material has been modeled here, which in reality would significantly reduce the plastic strains and hence the internal (strain) energy due to material deformation. However, it is to be noted that although the lower bound material data is pessimistic for the package, it would be optimistic for the integrity of any internal containment vessel due to a much more benign deceleration history upon impact.

All the elements identified with accumulated plastic strains need to be treated using this strain based approach to evaluate integrity.

It was initially intended that some “factor of safety” could be recommended on the “allowable” multi-axial strain enumerated using the R3 procedure. However, it would require much more extensive work than originally conceived. It is intended to progress with the objective and hopefully obtain some fruitful results, which would help to recommend such a factor in the near future.

It was also intended to compare the current assessment procedure with the elastic-plastic assessment for the “protection against local failure” approach in ASME VIII Division 2 (Ref. 5). It will be considered as a part of the ongoing work and is expected to be presented in the future.

ACKNOWLEDGMENTS

I hereby acknowledge valuable advice and editorial recommendations from my colleagues Iain Davidson and Danny Vince. I also hereby acknowledge some level of assistance from IDAC and Ansys - LS/Dyna technical support teams.

REFERENCES

1 International Atomic Energy Agency - Regulations for the Safe Transport of Radioactive Material, TS-R-1 2009 Edition
2 Ansys Inc. - Ansys 12.1 (PREP7) and LS/Dyna Explicit Finite Element Analysis tool
3 BSI - BS 1501:Part 1 1980, Steels for fired and unfired pressure vessels - Plate
4 BNFL - R3 Impact Assessment procedure, March 2003
5 American Society of Mechanical Engineers – ASME Boiler and Pressure Vessel Code, Section VIII, Division 2: Alternative Rules, Edition 2009